

## Temporal and Spectral Properties of Gamma-Ray Flashes

Hua Feng<sup>1</sup>, T. P. Li<sup>2,3</sup>, Mei Wu<sup>2</sup>, Min Zha<sup>2</sup>, and Q. Q. Zhu<sup>2</sup>

### ABSTRACT

The temporal and spectral properties of terrestrial gamma-ray flashes (TGFs) are studied. The delay of low energy photons relative to high energy ones in the  $\gamma$ -ray variations of the TGFs with high signal to noise ratio has been revealed by an approach of correlation analysis in the time domain on different time scales. The temporal structures of the TGFs in high energy band are usually narrower than that in low energy band. The spectral hardness has a general trend of decreasing with time in a flash. The observed temporal and spectral characteristics give constraints and valuable hints on the flash production mechanism.

### 1. Introduction

Intense  $\gamma$ -ray bursts of atmospheric origin were detected by the Burst and Transient Source Experiment (BATSE) detectors, located on the Compton Gamma Ray Observatory (CGRO) (*Fishman et al.*, 1994). All the observed TGFs were of short duration (a few milliseconds) and had extremely hard energy spectra consistent with bremsstrahlung radiation from energetic (MeV) electrons. Since they were spatially correlated with regions of high thunderstorm activity and in two cases have been correlated with individual lightning flashes (*Inan et al.*, 1996), they are thought to be caused by high-altitude discharges produced by runaway air breakdown. Several theoretical calculations have been done to explain the origins of TGFs under the runaway air breakdown mechanism (*Chang and Price*, 1995; *Taranenko and Roussel-Dupre*, 1996; *Lehtinen et al.*, 1996; *Lehtinen et al.*, 1997). The calculated  $\gamma$ -ray fluxes and duration of the bursts are comparable to those measured by the BATSE detector on the CGRO satellite.

As the runaway air breakdown is a fundamental new process in plasma, it is interesting to understanding more the physics of the process through studying TGFs, if they were truly caused by such a mechanism. Besides the total fluxes, durations and time-averaged spectra, the energy dependence of temporal profiles and spectral evolution of TGFs can give more information about

---

<sup>1</sup>Department of Engineering Physics, Tsinghua University, Beijing, China.

<sup>2</sup>Institute of High Energy Physics, Chinese Academy of Sciences, Beijing, China.

<sup>3</sup>Physics Department and Astrophysics Center, Tsinghua University, Beijing, China.

their production process. For this purpose we analyze the time-tagged event (TTE) data for TGFs observed by BATSE. For 4 energy channels with boundaries 25-55 keV, 55-110 keV, 110-320 keV, and  $> 320$  keV, the TTE data contains the arrival time ( $2\mu s$  resolution) of each photon from a triggered event up to  $\sim 3.3 \times 10^4$  photons. Of 47 TGFs observed on CGRO in  $\sim 4$  years and published by NASA in their details, 15 bursts with high signal to noise ratio are used in our analysis, which are selected by the criterion of  $F_m/T_{90} > 4 \text{ ph/cm}^{-2}/0.1\text{ms/ms}$ , where  $F_m$  is the peak rates of the counting series with time step 0.1 ms,  $T_{90}$  (ms) the burst duration which contains %90 burst photons.

## 2. Energy Dependence of Temporal Profiles

To study the energy dependence of temporal profiles, which is important to diagnose the emission mechanism, we construct two counting series  $f_1(t)$  and  $f_2(t)$  for each burst for the energy band 25-110 keV and  $> 110$  keV, respectively. The average pulse widths in the low and high energy bands and the relative time delays between the two bands can be calculated by a modified correlation analysis technique used in studying X-ray rapid variability of the black hole binary Cyg X-1 (*Li et al.*, 1999; *Li*, 2001).

The cross-correlation function of two time series  $f_1$  and  $f_2$  at time lag  $\tau$  is defined as

$$\text{CCF}(\tau) = \sum_i v_1(i\Delta t + \tau)v_2(i\Delta t)/\sigma(v_1)\sigma(v_2) \quad (1)$$

where  $v(t) = f(t) - \bar{f}$ ,  $f(t)$  is the number of photons in the time interval  $(t, t + \Delta t)$ ,  $\Delta t$  is the time step. If the function  $\text{CCF}(\tau)/\text{CCF}(0)$  has maximum at  $\tau = \Lambda$ , the time lag of the energy band 1 relative to the band 2 at the time scale  $\Delta t$  is then defined as  $\Lambda$ . Monte Carlo simulations have been done and the results show that with this technique we can measure the relative time delay between two bands over a wide range of time scale  $\Delta t$  with high time resolution. At large scales one usually can get enough signal photons in a time bin and desirable correlation values from finite time bins. And at small scales the effect of serious Poisson fluctuation of signal counts in a time bin can be compensated by the large amounts of time bin and accurate correlation values can also be derived with Eq. (1). A distribution of time lag vs. time scale can reflect the character of the physical process to produce the delay better than a single value of lag at only one time scale. A physical process usually occurs in a range of time scale, the spectral delay caused by the process should appear at different time scales, smoothly distributed in the range. On the other hand apparent delays from statistical fluctuation will fluctuate between positive and negative values.

For each studied burst and  $m = 25$  different values of time step  $\Delta t$  which are logarithmically uniformly placed in the region of  $10^{-5} - 10^{-3}$  s, we calculate the time lags  $\Lambda$  of  $f_1$  relative to  $f_2$ . All obtained time lags  $\Lambda_i$  ( $i = 1, \dots, m$ ) of each burst with high signal to noise ratio are always positive. We average each 5 successive  $\Lambda_i$  and show the distribution of average time lag vs. time scale in Fig. 1. The global average  $\bar{\Lambda} = \sum_{i=1}^m \Lambda_i/m$  and the standard deviation

$\sigma(\Lambda) = \sqrt{\sum(\Lambda_i - \bar{\Lambda})^2/(m-1)}$  for each selected TGF is listed in Table 1. The total counting profile and profiles in 4 energy bands of a TGF with BATSE trigger number 2955 are plotted in Figure 2, where the delay of lower energy photons relative to higher energy ones is apparent.

The width  $W_l$  of a temporal profile in a band  $l$  can be defined as the FWHM of the autocorrelation function

$$\text{ACF}(\tau) = \sum_i v_l(i\Delta t + \tau)v_l(i\Delta t)/\sigma^2(v_l) \quad (2)$$

The widths  $W_1$  and  $W_2$  of studied TGFs in the low and high energy bands are calculated and their ratios  $W_1/W_2$  are presented in Table 1, from which we can see that the lower energy pulses are wider than higher energy ones for most studied bursts.

### 3. Spectral Evolution

For two counts  $c_1$  in 25-110 keV band and  $c_2$  in  $> 110$  keV band recorded in the same time segment, we defined the hardness ratio as

$$h = \frac{c_2 - c_1}{c_2 + c_1} \quad (3)$$

To show the spectral evolution, a TGF's pulse is divided into 5 time segments, each segment contains approximately the same number of photons and the hardness ratio is calculated by Eq. (3). Figure 3 shows the spectral hardness variation vs. time (indicating by the segment number) with four panels grouped by the shape of temporal evolution of hardness. Although the shapes are various, a general trend of hardness that decreases with time appears in Fig. 3, which confirms the claim by *Nemiroff et al.* [1997] with earlier TGF data.

### 4. Discussion

For all the bursts with high signal to noise ratio we find that in comparison with high energy band of  $> 110$  keV,  $\gamma$ -ray variations in the low energy band of 25 - 110 keV are always late in the order of  $\sim 100 \mu\text{s}$ , pulses are usually wide, and the energy spectra have a general trend to softening with time. The above features of energy dependence of time profiles and spectral evolution observed in TGFs support models of runaway breakdown as they are naturally expected for  $\gamma$ -rays produced by explosive discharges in plasmas. Monte Carlo calculations show that large-voltage and high-temperature pinch plasma columns can generate observed  $\gamma$ -ray flashes with energy spectra and spectral evolution characteristics, including the magnitude of soft lags, consistent with those observed in  $\gamma$ -ray bursts (*Li and Wu, 1997; Li, 1998*).

Alternative mechanisms have been proposed to explain the origin of TGFs, e.g. *Fargion* [2001] claimed that TGFs originated from  $10^{15} - 10^{17}$  eV neutrinos of astrophysical nature induced air

showers and take TGFs as first evidences for discovering ultra high energy (UHE) neutrinos. Our Monte-Carlo simulations show that up-going air showers are hard to produce the observed time lags between hard and soft energy photons in TGFs. In our simulations a geometrical model of the earth, atmosphere and BATSE detector is set. High energy  $\gamma$ -rays initiated by UHE neutrinos are produced from the earth's surface, following with the up-going air showers. We tracked the secondary photons and electrons and record the arriving time and energy of all  $\gamma$ -rays reaching the detector, with deposition energy in the BATSE's region. Simulations were made with the Monte-Carlo package GEANT3 from CERN. In more than one thousand simulated bursts no time lag between hard and soft photons larger than  $10 \mu\text{s}$  has been found.

Quantitative comparison between observed features and expectations from models are needed to further confirm the mechanism and to study physics of the production process.

We thank Prof. Y. Muraki and the reviewers for helpful comments and suggestions. This study was supported by the Special Funds for Major State Basic Research Projects and by the National Natural Science Foundation of China and made use of data obtained through HEASARC Online Service, provided by NASA/GSFC.

## REFERENCES

- Fishman G. J., P. N. Bhat, R. Malozzi, J. M. Horack, T. Koshut, C. Kouveliotou, G. N. Pendleton, C. A. Meegan, R. B. Wilson, W. S. Paciesas, S. J. Goodman, H. atmospheric origin, science, *264*, 1313-1316, 1994.
- Chang B., and C. Price, Can gamma radiation be produced in the electrical environment above thunderstorms ?, *Geophys. Res. Lett.*, *22*, 1117-1120, 1995.
- Fargion D Horizontal and upward  $\tau$  air showers in valleys from mountains and space: Discovery UHE neutrinos and new physics, In *Proc. 27th Int. Cosmic Ray Conf.*, HE2.5, Germany, 2001 (also available in e-Print archive astro-ph/0106239)
- Inan U. S., S. C. Reising, G. J. Fishman, and J. M. Horack, On the association of terrestrial gamma-ray bursts with lightning and implications for sprites, *Geophys. Res. Lett.*, *23*, 1017-1020, 1996.
- Lehtinen N. G., M. Walt, U. S. Inan, T. F. Bell, and V. P. Pasko,  $\gamma$ -ray emission produced by a relativistic beam of runaway electrons accelerated by quasi-electrostatic thunder-cloud fields, *Geophys. Res. Lett.*, *23*, 2645-2648, 1996.
- Lehtinen N. G., T. F. Bell, V. P. Pasko, and U. S. Inan, A two-dimensional model of runaway electron beams driven by quasi-electrostatic thundercloud fields, *Geophys. Res. Lett.*, *24*, 2635-2638, 1997.

- Li T. P., Gamma-Ray Bursts from Electrical Discharges, *AIP Conf. Proc.* No.428 (Woodburg, NY: AIP), 825-829, 1998.
- Li T. P., Timing in the Time Domain: Cygnus X-1, *Chin. J. Astron. Astrophys.*, 1, 313-332, 2001.
- Li T. P., and M. Wu, Gamma-Ray Bursts from Discharges in Plasmas, *Chin. Phys. Lett.*, 14, 557-560, 1997.
- Li T. P., Y. X. Feng, and L. Chen, Temporal and Spectral Correlations of Cygnus X-1, *Astrophys. J.*, 521, 789-797, 1999.
- Nemiroff R. J., J. T. Bonnell, and J. P. Norris, Temporal and spectral characteristics of terrestrial gamma flashes, *J. Geophys. Res.*, 102, 9659-9665, 1997
- Taranenko Y., and Roussel-Dupre R., High altitude discharges and gamma-ray flashes: A manifestation of runaway air breakdown, *Geophys. Res. Lett.*, 23, 571-574, 1996.

Table 1 Selected TGFs

Trig No.	$T_{90}$ (ms)	$F_m(10^{-3} \text{ ph/cm}^2/0.1\text{ms})$	$F_m/T_{90}$	$\bar{\Lambda} \pm \sigma(\Lambda) (\mu\text{s})$	$W_1/W_2$
106	1.3	6.74	5.19	$102 \pm 28$	1.19
1433	1.5	7.15	4.77	$71 \pm 31$	1.64
2144	0.7	9.62	13.74	$115 \pm 40$	1.03
2348	1.1	7.15	6.50	$88 \pm 29$	1.04
2370	0.7	8.14	11.63	$151 \pm 29$	1.16
2465	1.0	7.89	7.89	$157 \pm 25$	1.38
2754	0.9	7.65	8.50	$120 \pm 29$	2.10
2808	1.0	5.67	5.67	$105 \pm 45$	0.88
2955	0.7	7.89	11.28	$125 \pm 21$	1.00
3377	1.0	10.11	10.11	$373 \pm 31$	1.47
5577	0.6	5.18	8.63	$81 \pm 33$	0.91
5587	1.2	6.41	5.34	$163 \pm 46$	1.16
5598	1.1	6.17	5.61	$117 \pm 20$	0.94
5665	1.4	7.65	5.46	$265 \pm 43$	1.54
6773	0.9	3.82	4.25	$278 \pm 61$	0.74

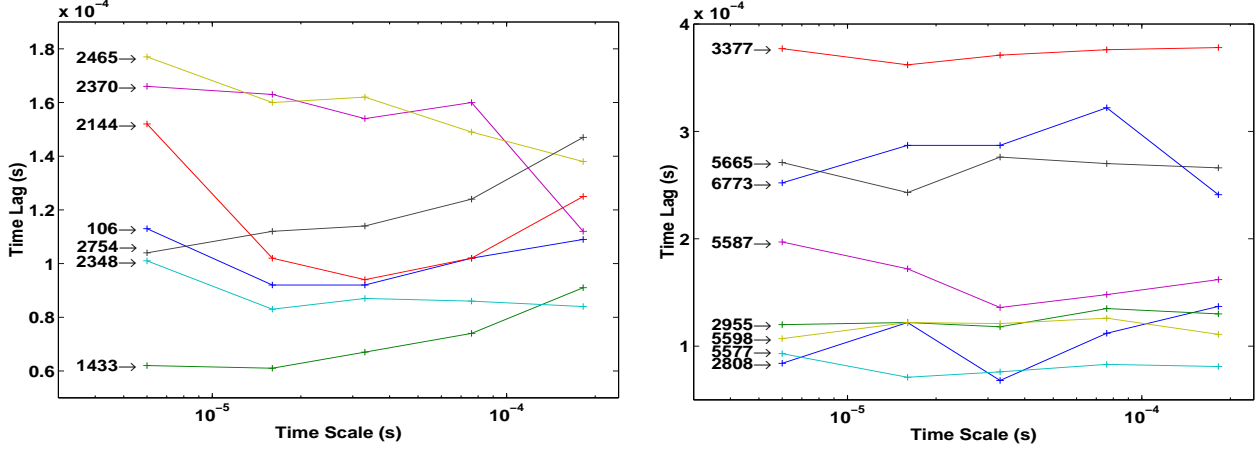


Fig. 1.— Soft  $\gamma$ -ray lag vs. time scale of TGFs. The quantity beside an arrow is the BATSE trigger number of the indicated burst.

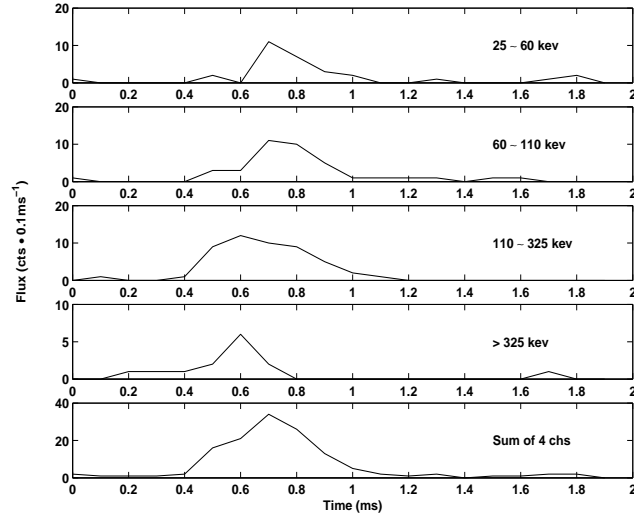


Fig. 2.— Counting rate profiles of a TGF with trigger number 2955 in different energy bands. From top to bottom is the profile in 25-60 keV, 60-110 keV, 110-325 keV,  $> 325$  keV and the total BATSE band, respectively.

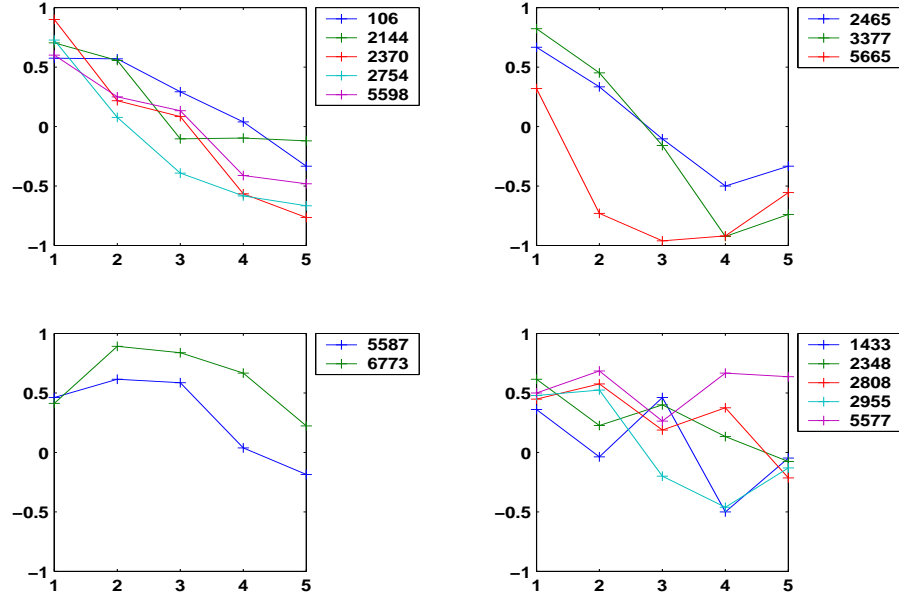


Fig. 3.— Spectral evolution of TGFs. The vertical axis is the hardness ratio defined by Eq. (3). The number marked along the abscissa is the segment number of a burst profile